Recent Improvements in Combustion Noise Investigation: from the Combustion Chamber to Nozzle Flow

Maxime Huet, François Vuillot, Nicolas Bertier, Thierry Poinsot, Marek Mazur, Nancy Kings, Wenjie Tao, P. Scouflaire, Franck Richecoeur, S. Ducruix, et al.

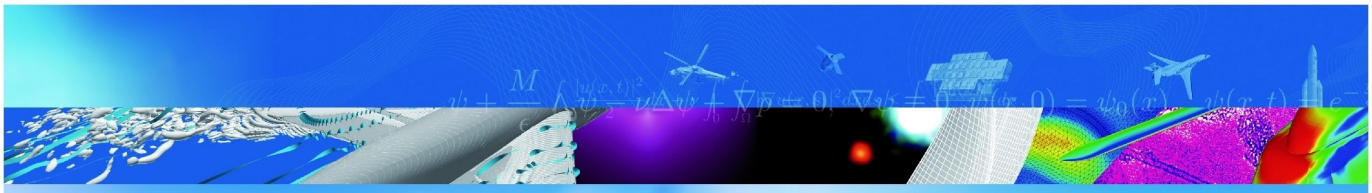

ARTICLE DE REVUE

Recent Improvements in Combustion Noise Investigation: from the Combustion Chamber to Nozzle Flow

M. Huet (ONERA), F. Vuillot (ONERA),
N. Bertier (ONERA), M. Mazur, N. Kings, W. Tao,
P. Scouflaire, F. Richecoeur, S. Ducruix,
C. Lapeyre, T. Poinsot

AEROSPACELAB JOURNAL

No 11, AL11-10, 17 pages

TP 2016-556

70 2016 ans

ONERA

THE FRENCH AEROSPACE LAB

M. Huet, F. Vuillot, N. Bertier
(ONERA)

M. Mazur, N. Kings, W. Tao, P. Scouflaire, F. Richecoeur, S. Ducruix
(Laboratoire EM2C, CNRS, Centrale Supélec, Université Paris-Saclay)

C. Lapeyre, T. Poinsot
(Institut de Mécanique des Fluides de Toulouse)

E-mail : maxime.huet@onera.fr

DOI : 10.12762/2016.AL11-10

Recent Improvements in Combustion Noise Investigation: from the Combustion Chamber to Nozzle Flow

For a long time, engine noise has been dominated by fan and jet noise. With their reduction for modern turbojets, for instance, combustion noise is no longer negligible and efforts are concentrated on its understanding. The objective of the European project RECORD is to help to understand the fundamental mechanisms of core noise, in order to reduce it. In this paper, the recent advances achieved within the project for the noise generated through a nozzle are presented. This work includes the definition of a combustion test bench at the EM2C laboratory, equipped with various diagnostic techniques and an outlet nozzle to pressurize the chamber and generate entropy noise. Reactive simulations of this facility are performed by ONERA and CERFACS using LES. Finally, simulated flow fields are post-processed to determine direct (acoustic) and indirect (entropy) contributions to the global noise generated by the nozzle. This work is a first step before the modeling of a full engine, including the turbine stages.

Introduction

With increasingly severe environmental regulations, noise pollution is now a major concern for aircraft operators. Among all of the noise sources of an aircraft, engine noise is the major contributor and much attention remains focused on its reduction. For a turbojet engine, jet and fan noise are the dominant noise sources and, as such, have been the subject of great efforts for their reduction by the aeroacoustics community over the last decades. In modern engines, additional noise sources that were previously masked by those two main contributors can no longer be neglected, and may even become predominant for specific frequencies and operating points. As illustrated in Figure 1, this is the case for the combustion noise in the medium frequency range at the approach regime [1].

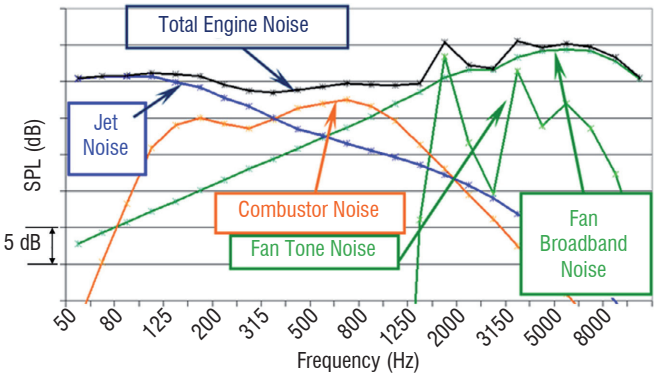

Figure 1 - Typical contribution of turbojet engine noise sources on approach, from SAFRAN Snecma [1]

The contribution of combustion noise was first evidenced in the 1970s with the engine noise being found to be higher than the sole contribution of the jet [2]. Being first referred to as excess noise [3], this additional noise was then associated with the combustion process and is now called core noise [4] or combustion noise [5]. First theoretical analyses where provided by Bragg [6] and Strahle [7] and this noise was shown to have two distinct origins. Pressure fluctuations can be generated by the unsteady heat release of the flame; it then corresponds to direct noise [6]-[13]. The unsteady turbulent flame also generates temperature (entropy) and velocity (vorticity) perturbations that create additional noise when accelerated by the mean flow through a nozzle or a turbine. The latter is called indirect noise [14]-[16]. Marble and Candel [17] were among the first to quantify the noise generated by small-amplitude entropy spots convected through a compact nozzle, where the wavelengths are assumed to be large compared to the considered geometry. Their approach was later extended to entropy and vorticity spots passing through turbine rows by Cumpsty and Marble [18].

Under normal operating conditions, the noise sources are incoherent and radiate a broadband of frequencies. For particular configurations, however, a coupling may appear between the fluctuations emitted by the flame and the boundaries of the combustion chamber and lead to combustion instabilities [19]-[22] with very high tonal noise that may even cause the destruction of the combustor. Recent studies showed the role of accelerated entropy spots on the onset or sustainability of these instabilities [23]-[28], highlighting the importance of understanding the basic mechanisms of combustion noise and its prediction. Combustion instabilities are however beyond the scope of this paper and will not be discussed. The reader can refer to the surveys

by Candel *et al* [29] and McManus *et al* [30] for a more detailed view of the state of knowledge in the field of combustion noise.

An illustration of the evaluation of combustion noise in modern aero-engines is proposed by Duran *et al* in an earlier issue of the journal [31]. In their paper, the authors focused on the direct and indirect combustion noise mechanisms. Reference experimental facilities (an entropy noise test bench [32] and an instrumented full-scale turbo-shaft engine [33], [34]) are also detailed and a numerical evaluation of combustion noise is illustrated for a model engine composed of a combustion chamber and turbine stages.

Recently, European research activities on the topic have been concentrated through the RECORD project, funded by the European Union [35]. The objective of the project is to aid in the understanding of the fundamental mechanisms of core noise generation and to propose ways to reduce it. To this end, experimental facilities, numerical simulations and analytical models are being set up to cover all of the stages of direct and indirect noise generation. The experimental activities consist, in detail, in the injection of acoustic and entropy waves through a nozzle for the evaluation of nozzle transfer functions [36], [37], in an instrumented pressurized combustion chamber with a one-stage swirl injector [38] and in a high-pressure turbine stage that can be fed with acoustic, entropy or vorticity waves [39].

This paper presents the recent advances achieved during the RECORD project with regard to the experimental evaluation and numerical prediction of combustion noise generated inside a combustion chamber equipped with a nozzle at its outlet. It combines experimental results on a dedicated combustor, unsteady reactive numerical simulations of the facility and analytical models to evaluate direct and indirect combustion noise. Measured, simulated and modeled results are cross-compared for validation and the contribution of acoustics and entropy perturbations to the noise generated in the combustor is evaluated. The paper is organized as follows. The experimental facility is described in a first step; the diagnostic techniques and operating points are particularly discussed. Numerical simulations reproducing the flame and its noise generation are presented in a second step. The acoustic post-processing of the simulations is then detailed. This section includes the methodology of wave extraction from the CFD fields and the evaluation of noise generation through the nozzle. The paper finally ends with conclusions and perspectives.

Experimental facility

The CESAM-HP Test bench for stabilizing a lean flame in a pressurized chamber

The CESAM-HP test bench was developed at the EM2C Laboratory with the aim of studying combustion noise and its contributors – direct and indirect combustion noise. Having been designed within the framework of the RECORD project, it features a one-stage swirl injector, a combustion chamber with large optical accesses and an exhaust nozzle used to pressurize the combustion chamber and generate indirect noise. Figure 2 shows a schematic drawing of the CESAM-HP test bench.

The test bench comprises the following elements:

- The Impedance Control System (ICS), consisting of a perforated plate with a bias air flow, which in connection with an adjustable cavity can be used to damp instabilities at a chosen frequency. The system has been developed as part of prior work at the EM2C Laboratory [40],[41]. The axial flow is also aimed at limiting the flame flash back. It can be balanced between a high-speed central jet and a lower speed flow going through the piston. This distribution of the air flow influences acoustic behavior on the test bench, as will be shown below.
- The injection system, consisting of one tangential stage where the air/propane premixture is injected. The tangential injection ensures a strong swirling motion, which results in a compact flame that can be operated in lean conditions.
- The square section chamber (70 mm × 70 mm × 140 mm), featuring top and bottom cooled walls, and a large optical access on one side. The last wall bears the ignition system and the pressure and temperature instrumentation. The test bench modularity enables the walls and glass window to be exchanged, depending on the diagnostic technique applied.
- The exhaust nozzle downstream of the combustion chamber, aimed at increasing the mean pressure and increasing the burnt gas velocity. At the operating points studied, the nozzle is choked and the chamber pressure rises to over 2 bars. The nozzle shape was acoustically optimized, in order to generate a maximal amount of entropy noise. This is done by describing the nozzle shape with several Bezier splines and by applying a genetic algorithm for optimization. [42]

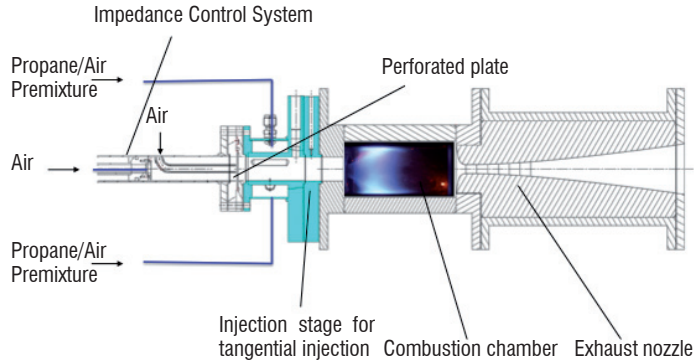

Figure 2 - Schematic drawing of the CESAM-HP test bench

Diagnostic techniques for measuring the dynamic properties of the flow

Various diagnostic techniques are used to quantify the flow properties and acoustics during operations. A schematic drawing of the combustion chamber in Figure 3 shows the various sensor positions.

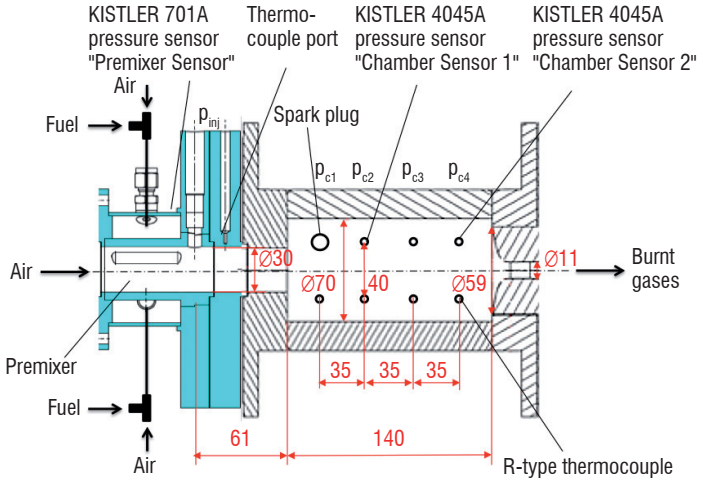

Figure 3 - Schematic drawing of the combustion chamber with its feeding lines and various sensor positions

Pressure measurements are performed on the test bench. Due to the pressurization of the test bench, piezo-resistive sensors (KISTLER 4045A) are installed directly in the chamber walls and can simultaneously measure the static pressure and dynamic pressure fluctuations. A reliable, stable and long-time operation is ensured by the integration into a combined system of thermal protection and water-cooling, made as part of previous work [43],[44],[45]. The dynamic pressure fluctuations in the injector are measured by dynamic-only sensors of the type KISTER 701A. The pressure evolution is recorded during operation for 4 s, with a sampling frequency equal to 25 kHz.

Thermocouple measurements are performed at several positions of the test bench for monitoring purposes, but also inside the combustor for global characterization. While slow in response, the R-type thermocouple installed in-chamber is able to measure temperatures up to 1600 °C and is therefore suitable for the measurement of the temperature of burnt gases.

Three operating points to test different injection strategies

For all of the operating points, most of the mass flow enters the chamber through the tangential injection, in order to guarantee an intense swirling motion. The axial mass flow comes either from the central orifice (at high-speed) or goes through the perforated back plate (at lower speed). The balance between the two axial injection systems has a significant influence on chamber acoustics. Among a large variety of possible operating points, three have been retained for their interest from an acoustic point of view. Their properties are summarized in Table 1.

Property	Values		
Name	op16-0-2-85	op16-2-0-85	op13-5-0-85
Fuel type	Propane	Propane	Propane
Fresh fuel and air temperature [°C]	20	20	20
Tangential air flow rate [g/s]	16	16	13
Tangential fuel flow rate [g/s]	0.968	0.968	0.968
Central jet air flow rate [g/s]	0	2	5
Piston air flow rate [g/s]	2	0	0
Global equivalence ratio	0.85	0.85	0.85
Power [kW]	44.9	44.9	44.9
Mean chamber pressure [bar]	2.02	2.02	2.01

Table 1 - Main properties of the studied operating points

For each operating point, we propose here to present the acoustic spectra that synthesize the dynamics at work in the chamber. Once the stable regime is reached, the dynamic pressure at the walls is recorded and power spectral densities are computed using Welch's periodogram method with segments of 2048 samples, Hamming windows and a 50% overlap. The resulting spectra are shown in Figure 4.

All of the spectra contain both a broadband acoustic power and some resonant peaks. This illustrates two phenomena at work: a large band noise and combustion instabilities. The proportion of each changes with the injection strategy.

The spectra of op16-0-2-85 and op16-2-0-85 are dominated by a low frequency peak around 120 Hz and its harmonics. Theoretical work determined that these are related to the feeding lines [38]. For point op16-0-2-85, the higher harmonics are slightly damped, but the change in the air injection location (through the back plate or through the central hole) does not strongly modify the power spectrum.

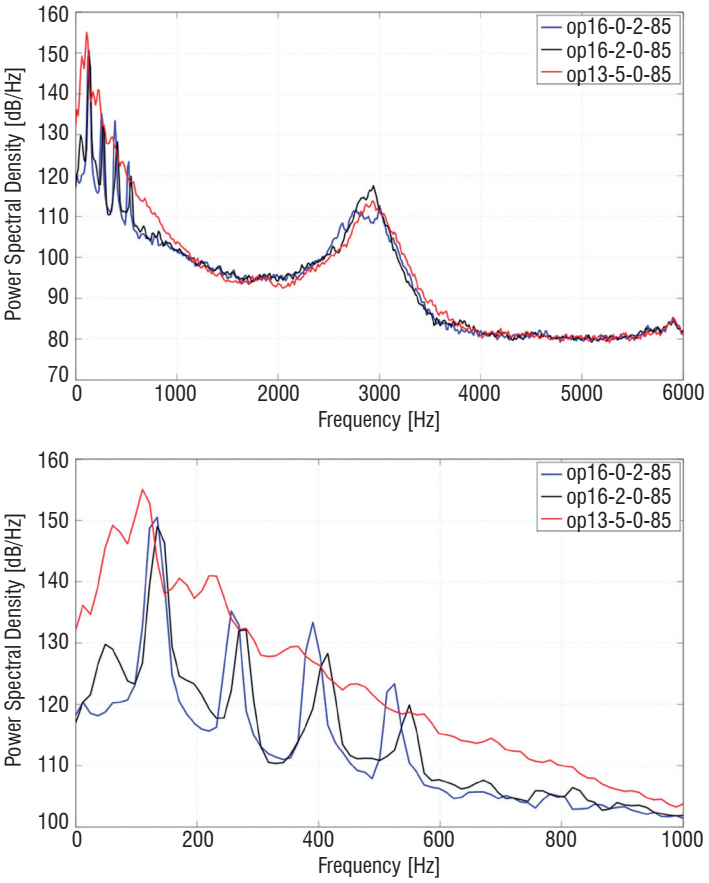

Figure 4 - Power Spectral Density of the three operating points, with a magnified view in the low frequency area at Sensor Position 2

For operating point op13-5-0-85, instabilities barely exist and a broadband low frequency peak is observed.

Most of the dynamics are concentrated under 1 kHz. At higher frequencies, all of the pressure spectra feature the same increase in amplitude around 3 kHz, potentially corresponding to a higher mode. However, contrary to what would be expected for an eigenmode, the peak is large and this might be associated with measurement noise. Further experimental results concerning the analysis of eigenmodes and eigenfrequencies are presented by Mazur *et al* [46] and Kings *et al* [47]. The purpose of this study is to describe additional diagnostic and processing tools that are necessary to point out the potential acoustic sources in the chamber.

Numerical simulations

In order to identify the sources of combustion noise, the decision was made for the RECORD project to support High Fidelity compressible Large Eddy Simulations (HFLES) of the experimental setup CESAM-HP from the EM2C (see above). These simulations were intended to provide detailed insight into the flow and combustion processes acting in the pressurized one-stage combustion chamber. Two HFLES compressible codes were used to conduct simulations of this setup: the AVBP code, which was used in collaboration by both CERFACS and EM2C; and CEDRE, which was used at ONERA. These codes present valuable differences in their numerical contents and

modeling approaches and have demonstrated their ability to represent such complex reacting flows involving strong interactions between unsteady fluid dynamics, acoustics and combustion. Moreover, compressible LES codes are very well suited for this study, since they enable the choked nozzle and sonic throat to be naturally included in the computations. This enables the unsteady behavior of the domain outlet to be fully reproduced, including acoustic impedance and full 3D effects. Finally, having two codes with different numerical approaches permitted very useful cross-calculations, which helped to finalize the experimental set-up definition and to choose appropriate operating points.

In the course of the RECORD project, several computations were performed by both teams on different configurations and helped to understand the strong unstable behavior of the initial set-up with a two-element injector. Once a proper operating point was established, both cold and reacting computations were performed and compared to the experiment for the reference one-element configuration. Only the reacting case results are presented here.

Code description

AVBP

The compressible Large Eddy Simulations of the CESAM-HP burner were conducted with the high-fidelity LES code AVBP [48]-[50] developed by CERFACS and IFP-EN. AVBP solves the 3D compressible Navier-Stokes equations using both DNS and LES approaches on unstructured and hybrid meshes. The numerical scheme in AVBP relies on the Cell Vertex (CV) Finite-Volume (FV) method [50]. The third-order in time and space Taylor-Galerkin Finite Element scheme TTGC [51] was used in the simulations for its accuracy on the propagation of vortices and acoustic waves. Turbulence on the subgrid scale was handled by the Sigma model [52]. Combustion kinetics were described by a global one-step reaction including five species (C_3H_8, O_2, N_2, CO_2, H_2O), while the turbulence-combustion interaction was described by the Dynamic Thickened Flame model [53] combined with the Charlette-Meneveau efficiency function [54]. The boundary conditions were implemented with the Navier-Stokes Characteristic Boundary Conditions (NSCBC) [55]. Specific heat resistances matching the cooling power applied on individual walls during the experiments were used to treat heat losses on these chamber walls. The flow through the perforations of the back plate was not resolved, due to its high computational cost. Instead, the perforated plate was replaced by a coupled boundary condition giving a uniform acoustic treatment based on the instantaneous pressure drop through the perforated holes. This approach, developed in [56], is aimed at recovering the frequency-domain acoustic impedance of the perforated plate in time-domain LES simulations.

CEDRE

The CEDRE code is being developed by ONERA for energetics and propulsion research and applications [57]-[61]. It is a fully parallel multi-physics code that relies on dedicated solvers for resolving various physical systems. In this work, only the gas phase solver CHARME has been used. It solves the compressible reactive multi-species Navier-Stokes equations on generalized unstructured meshes (polyhedra). It provides a zonal modeling approach based on user domain decomposition, where particular models can be activated. It is based on a finite volume cell-centered MUSCL approach, combined with explicit or implicit time integration. Space and time numerical schemes can be combined up to the fourth order in space and time [62]. Based on previous experience, these computations were carried out with a choice of second order space schemes, combined with a one-step implicit GMRES time integration. In order to capture the acoustic waves, CFL numbers were kept close to unity over most of the computational domain. The CHARME solver allows choosing among varied turbulence models, from RANS to LES, including hybrid approaches such as DDES or ZDES [60], [63]. All turbulence models can be completed by particular laws of the wall, which are activated when required by the grid resolution at the walls. Wall thermal conditions were imposed by approximated experimental conditions, as provided by the EM2CS team. These computations were run using the Smagorinsky LES model. Lean combustion enables the use of global combustion kinetics involving only five species (C3H8, O2, N2, CO2, H2O). For subgrid turbulence-combustion interaction, a Dynamic Thickened Flame model was used in conjunction with the Charlette efficiency function [54]. A controlled acoustic condition was used to represent the behavior of the ICS. It used a particular boundary condition available in the CEDRE code to represent in the time domain the complex acoustic impedance of the ICS, as measured by the EM2C team. This condition is based on previous work [64], [65].

Geometry and grids

The numerical test case for the modified CESAM-HP setup is described in Figure 5. It includes the entire swirled one-element tangential injection system, the pressurized chamber, and a part of the experimental nozzle truncated after the sonic throat. The rest of the diverging section of the nozzle is not included in the domain, since it is not needed to capture the sonic nozzle acoustic response for the reflected noise. However, it will be considered in some of the acoustic analysis (transmitted noise). The origin of the reference axes is set at the center of the plenum exit (dump plane), with the x-axis oriented in the direction of the flow (Figure 5).

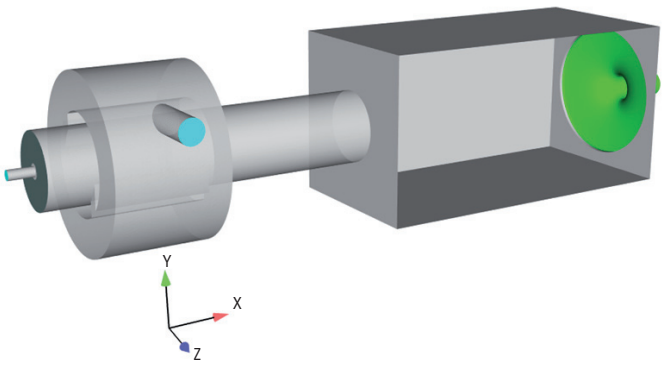

Figure 5 - Computational domain

One operating point was selected from the experimental data base and is summarized in Table 2. The inlet stagnation temperature is set at 290 K.

Operating point	Air MFR injection stage	Air MFR axial jet	Air MFR ICS	Overall equivalence ratio
OP13-5-0-85	13 g/s	5 g/s	0 g/s	0.85

Table 2 - Experimental operating conditions

The geometry and first grid used were built by CERFACS from the CAD file provided by EM2C team and are shown in Figure 5. The grids were generated with the Centaur mesh generator [66]. The nozzle divergent section is not fully meshed, since the nozzle will be choked for the reactive computations. A sufficient part of the divergent has been included, for the sonic line to always be in the computational domain.

Two similar meshes were used by ONERA and CERFACS for this geometry. Figure 6 shows the mesh used by ONERA, which ranges from the ICS to the nozzle divergent. Figure 7 shows the computational domain used by CERFACS, including the ICS. The CERFACS mesh is a fully tetrahedron unstructured mesh. The ONERA mesh was derived from the CERFACS mesh, to introduce three separate domains: Plenum/Injection, Chamber and Nozzle. It includes prisms along the nozzle walls and at the Plenum-Chamber interface. The main characteristics of these meshes are summarized in Table 3.

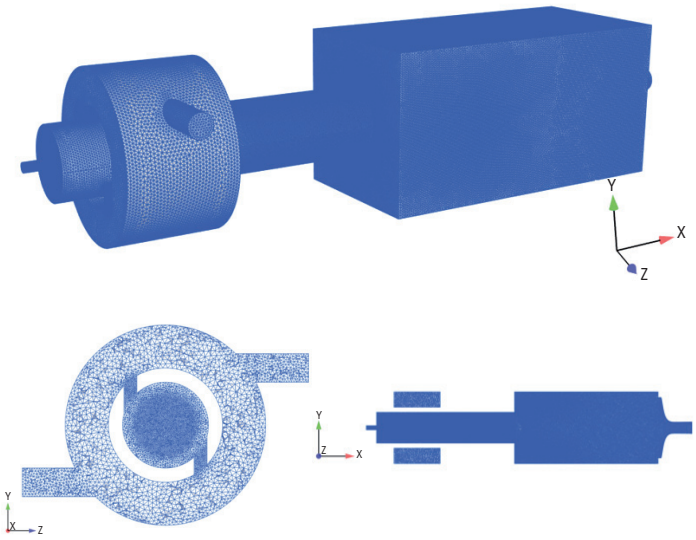

Figure 6 - Mesh used by CEDRE

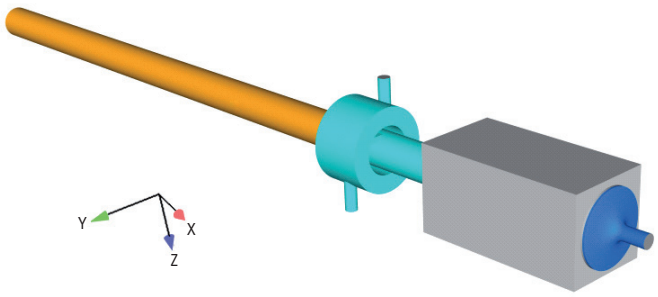

Figure 7 - Final mesh used by AVBP

A controlled acoustic condition was used to represent the behavior of the ICS, as mentioned previously. ONERA used a particular boundary condition available in the CEDRE code to represent in the time domain the complex acoustic impedance of the ICS, as measured by the EM2C team. A different approach was used by CERFACS, where the chamber upstream of the ICS was meshed and a coupled strategy was used to model the plate behavior. The capabilities of this approach in reproducing the actual impedance have been demonstrated before, with the AVBP code [56]. The proper treatment of the acoustic response of the ICS device appeared to be essential in the final results and both approaches provided satisfactory results.

Mesh	No. of cells	Element types	No. of domains
CERFACS	10.9 M	tetrahedra	1
ONERA	11.1 M	tetrahedra, prisms, pyramids	3

Table 3 - Main characteristics of the meshes

Finally, the main numerical parameters for the two codes are summarized in Table 4.

Code	Space discretization	Temporal integration	Time step
CEDRE	MUSCL (O2)	Implicit: backward Euler	1e-6 s
AVBP	TTGC (O3)	Explicit: RK2	1e-7 s

Table 4 - Numerical set-up

Results

The preliminary results from both teams had shown a strongly unstable behavior with marked flashback situations. Controlling this behavior involved several adjustments in the numerical set-ups. In particular, the proper handling of the ICS boundary condition appeared to be essential, as mentioned above. Additional adjustments were also performed and involved additional damping boundary conditions (AVBP) or modular treatments of the various zones of the computational domain (CEDRE). Concerning the CEDRE computations, a preliminary solution was obtained before the full ICS boundary condition was available, by simply de-activating the combustion in the Plenum/injection domain. This proved to be very efficient in suppressing flashback situations and provided interesting results. This computation will be referred to hereafter as the "-n" computation. However this simple solution lacked an important feature of the experiment, since the large low frequency motion was absent from this simulation. Once the ICS acoustic impedance was introduced into the computation, this simplified solution was completed by a fully reacting solution. This computation will be referred to hereafter as the "-b4n2" computation. Both solutions will be presented, since they provide interesting insight into the complex interactions between flow features, acoustics and combustion. The study of the flashback phenomenon in the CESAM-HP experiment is presented in reference [67]. Further details about the AVBP computations performed for this experiment can be found in the PhD theses of Lapeyre and Tao ([68], [69]).

Mean flow

The computed mean temperature fields are illustrated in Figure 8 for the three available computations. It can be noted that the AVBP and CEDRE "-n" computations provide similar mean temperature fields, where the plenum region is mostly unaffected by the flame, exhibiting low temperature levels. On the contrary, the CEDRE "-b4n2" computation shows that a relatively high temperature is observed in the plenum domain, due to marked low frequency motion of the flame across the dump plane. In Figure 8 d) numerical profiles are compared to measurements at the position X = -95 mm inside the plenum. This figure indicates that the results of the "-b4n2" computation are compatible with the measured temperature in the plenum, indicating that flame motion is indeed present in the experiment and leads to increased temperature levels in this region.

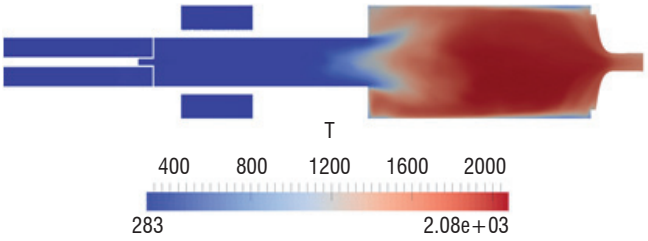

a)

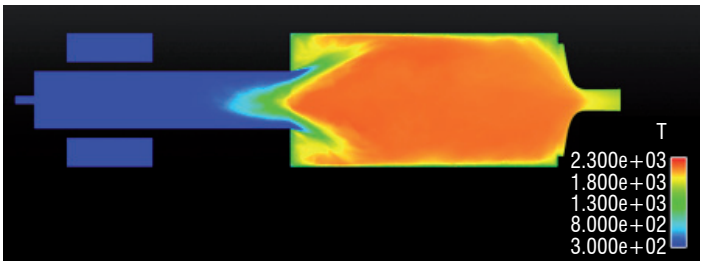

b)

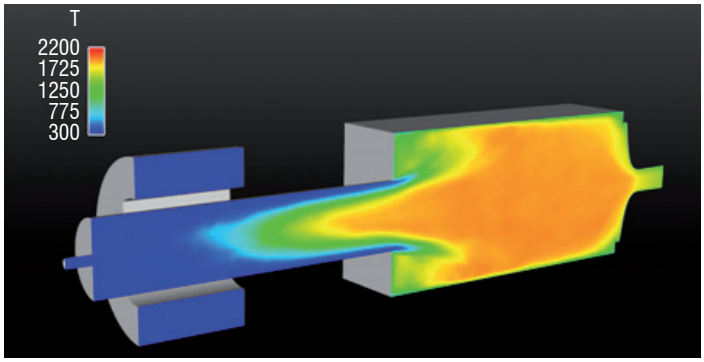

c)

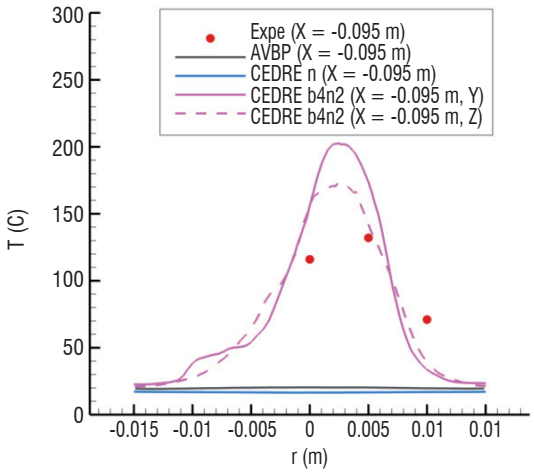

d)

Figure 8 - Mean temperature fields (K). From left to right and top to bottom, a) AVBP computation, b) CEDRE "-n" computation, c) CEDRE "-b4n2" computation, and d) comparison to measurements inside the plenum (x=-0.095 m)

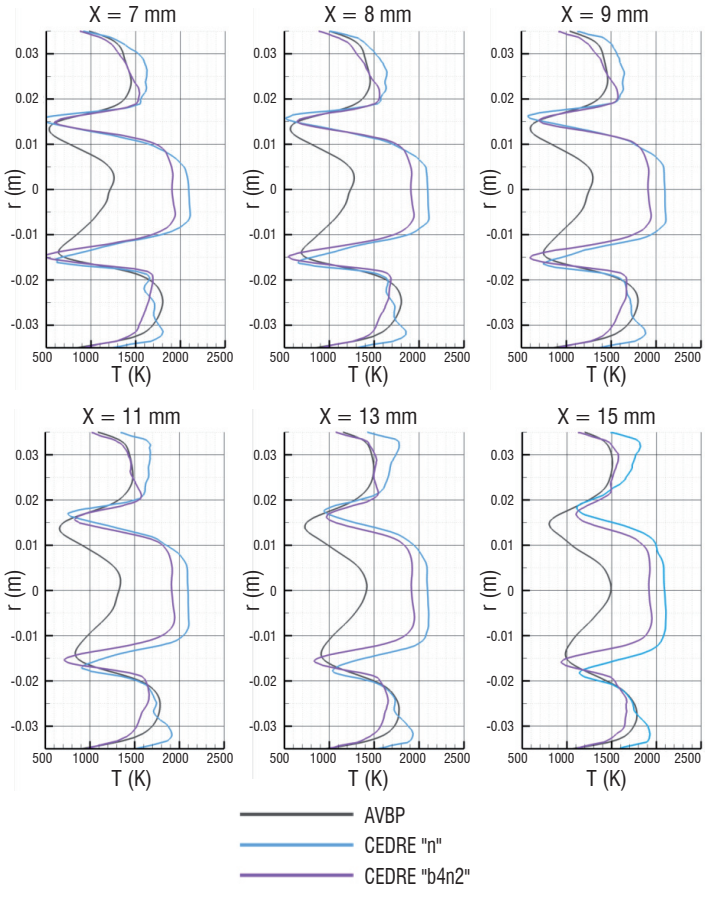

Figure 9 - Mean temperature profiles at the dump plane

Despite no other experimental mean temperature data being available, it is interesting to look at the computed mean temperature profiles in the combustion chamber. In the dump plane region (Figure 9), it appears that the AVBP computation shows a slower flame development, with a narrower angle, compared to both CEDRE computations. At the chamber exit (Figure 10), all computations recover, as expected, very similar levels of mean temperature approaching the equilibrium temperature (Teq = 2131.7 K). Please note that, since the grid used does not resolve the boundary layers, the mean temperature gradients that are visible in Figure 10 are not representative of the wall thermal boundary conditions, but rather of the complex flow structure that develops in the combustion chamber. Nevertheless, all of the computations were performed with suitable thermal boundary conditions reproducing the experimental heat losses at the various walls, which were water cooled except for the window wall, which was treated as an adiabatic wall. No marked influence of the wall thermal conditions on the unsteady flow was observed in the various computational results obtained during the RECORD project.

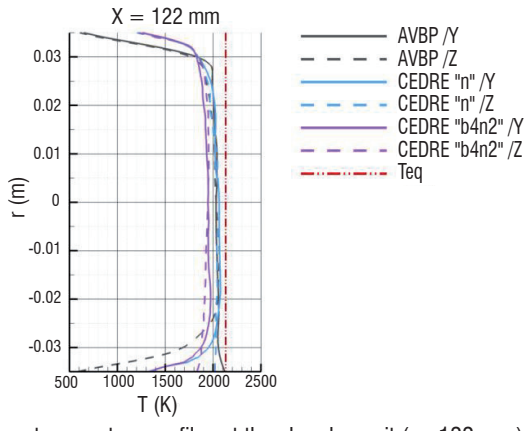

Figure 10 - Mean temperature profiles at the chamber exit (x=122 mm)

Figure 11 offers global comparisons of the mean and rms velocity fields between the "-b4n2" computation and the available PIV measurements performed on the test-bench, but these are not further presented here. This figure shows that an overall good comparison of the flow feature is recovered. However, it must be noted that the axial oscillations at the dump plane (rms plot) are stronger in the LES "-b4n2" computation than in the measurements.

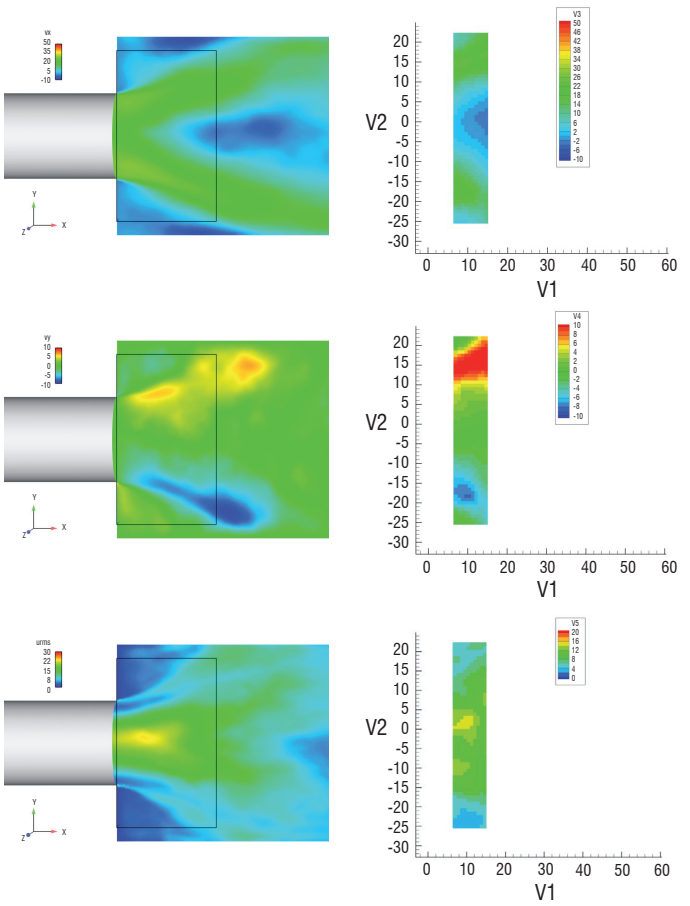

Figure 11 - Comparison of the mean and rms velocity fields. Computation "-b4n2" (left), experimental PIV (right). From top to bottom: Vx, Vy, Urms. The same color scale is used, except for the rms plot.

Detailed comparisons

Concerning cross calculations, a detailed comparison was performed using the profiles defined in Figure 12.

This section offers some comparisons of the LES computations to the available measurements for OP13-5-0-85. Figure 3 illustrates the experimental set-up and probe locations. Figure 12 illustrates the axial locations of the transverse profiles.

First, the time signal and its PSD at experimental Pressure Transducer 2 (see Figure 3) are presented in Figure 13. In this figure, the difference of the mean pressure level between computations and experiment is visible. This difference is due to nozzle erosion in the experimental set-up. Further, the absence of strong low frequency oscillations in the ONERA "-n" computation is also visible. Concerning the CERFACS/EM2C and the ONERA "-b4n2" computations, it is noted that both computations recover the low frequency oscillations, in good agreement with the experimental results. The PSD plot confirms this good agreement. It must be noted that the ONERA "-b4n2" computation slightly over-estimates this oscillation.

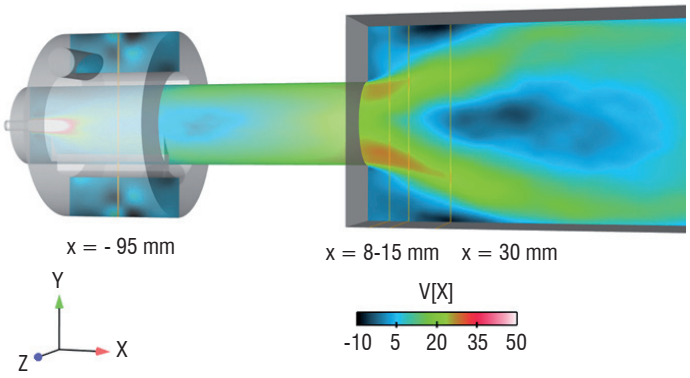

Figure 12 - Extraction planes for profile comparisons

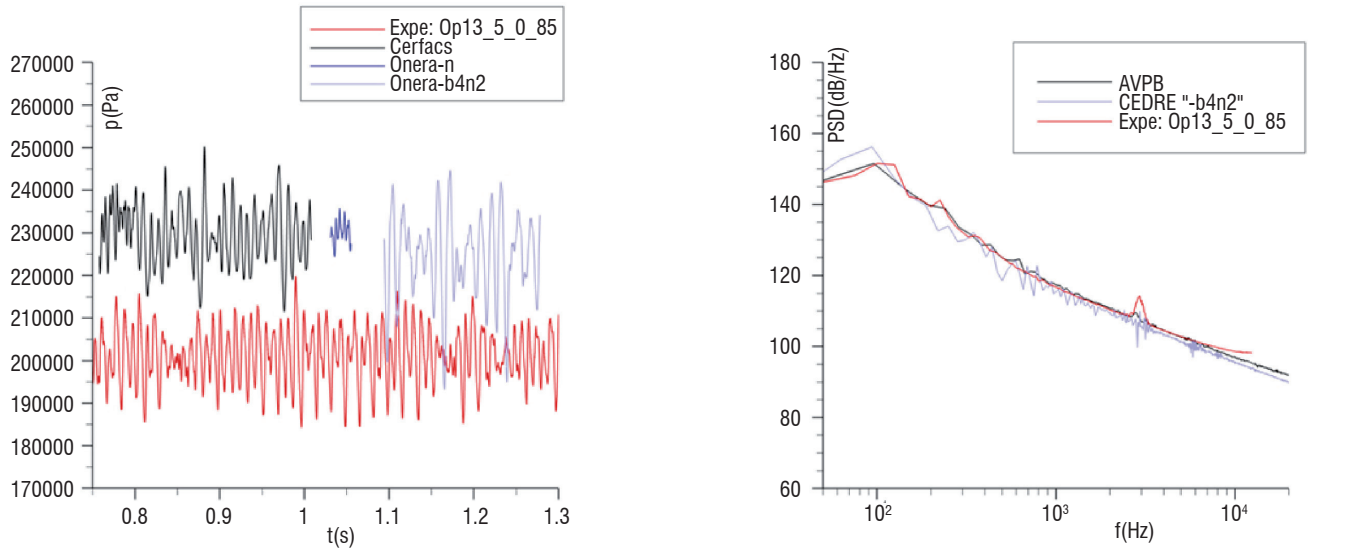

Figure 13 - Time signal (left, arbitrary time origin) and PSD (right) at Transducer 2

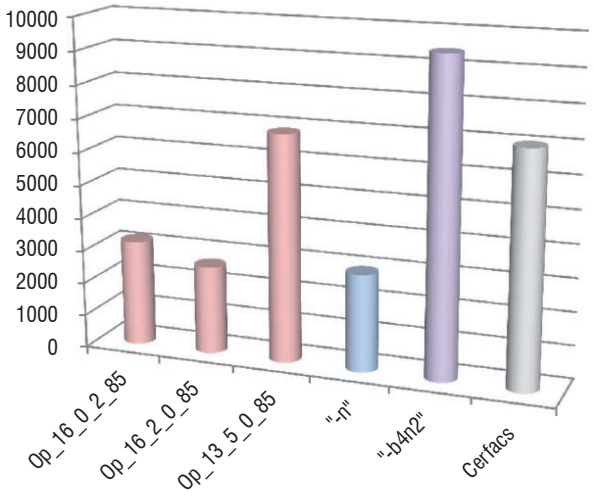

Figure 14 - RMS pressure at Transducer No. 2 (Pa)

The computed rms pressure at Transducer 2 is compared to available experimental data in Figure 14. This figure confirms the fact that the low-frequency high-amplitude oscillation is present in the Op_13_5_0_85 experiment and is recovered by the AVBP and CEDRE "-b4n2" computations, while the CEDRE "-n" computation produces much reduced levels comparable to the other experimental point. This enables the low-frequency oscillation to be linked to the flame motion across the dump plane, which implies burning inside the Plenum/injection domain.

Figure 15 (next page) presents the comparison of the computational results with available 2D PIV measurements at the dump plane region.

From Figure 15 it appears that the experimental profiles at the dump plane are difficult to perfectly recover from the computations. However, it can be noted that the ONERA "-n" computation shows very good mean velocity profile comparisons, while underestimating the rms levels. On the contrary, the "-b4n2" computation overestimates the rms levels and the mean profiles are not fully recovered. The CERFACS/EM2C computation, while achieving good agreement on the rms plots, shows marked discrepancies with the mean profiles, with a different flow cone angle. These results illustrate the difficulty in fully recovering the experiment in one computation, while overall agreement is deemed to be quite satisfactory from the pressure signals and frequency content.

Intermediate conclusion on HFLES results

The results show very favorable comparisons with experimental data. One noted difficulty was observed in the mean velocity profiles, just downstream from the dump plane (the first 15 mm), where the PIV measurements were available. In this limited region, the comparison work exhibited different results from the three analyzed computations, with difficulties in exactly recovering at the same time both the mean and rms profiles in one computation. However, the set of the three available computations well bracketed the measurements. Nevertheless the more global comparisons show that the computations correctly recovered the main flow features. Obviously, the difficulty lays in properly capturing the large-amplitude, low-frequency flame motion across the dump plane, moving in and out of the plenum domain. Under such conditions, the flashback phenomenon had to be controlled in the computations and the role of the ICS impedance turned out to be a key element in this process. Both codes could attain this result with different approaches. In such a complex situation, it is remarkable that both codes produced results in close agreement with the measurements, as illustrated by the time signal and PSD computed at Pressure Sensor 2 and by the temperature data in the plenum domain. This gives good confidence in the ability of the HFLES approach to describe complex combustion chamber phenomena.

Acoustic post-processing

Experiments or unsteady reactive numerical simulations provide the pressure and temperature fluctuations generated by the flame inside the combustion chamber. In the present case, the objective of the post-processing is, as a first step, to separate the waves (acoustic and entropy) present inside the chamber and, as a second step, to evaluate their relative contribution to the noise emitted by the nozzle and that goes back inside the chamber or enters the turbine stages that would be present in a real engine. A similar post-processing, with the propagation of noise and entropy waves through fixed and rotating blades of a compact turbine (low frequency limit) in order to compute the combustion noise generated at the outlet, has been performed by Duran *et al* [70]. In the following, an illustration of the post-processing is given using the CFD data presented in the previous section. With the current tools, it is assumed that the acoustic and entropy fluctuations, as well as the mean flow through the nozzle, are one-dimensional.

Wave extraction from CFD

The first step of the acoustic post-processing is the evaluation of the acoustic and entropy perturbations computed inside the combustion chamber. The determination of these waves is performed through a characteristic filtering [71], the principle of which is to separate the waves using their different propagation velocities. Instantaneous pressure, velocity and temperature fluctuations are stored on several planes downstream from the flame location, where the waves are supposed to propagate without source or damping terms, see Figure 16.

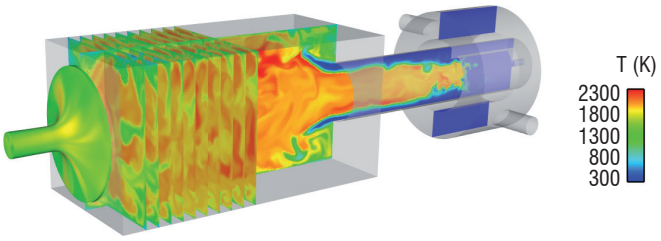

Figure 16 - Illustration of the storage planes used for the wave separation (the actual storage is performed on 20 planes)

Due to the three-dimensional, turbulent nature of the flow in the region downstream from the flame, the wave separation is achieved in three steps. First, a spatial averaging (area averaging) of the fluctuations is performed for each plane and at each time step, in order to construct 1D perturbations. By doing so, only the fluctuations corresponding to the planar waves are conserved, while the contributions of the higher

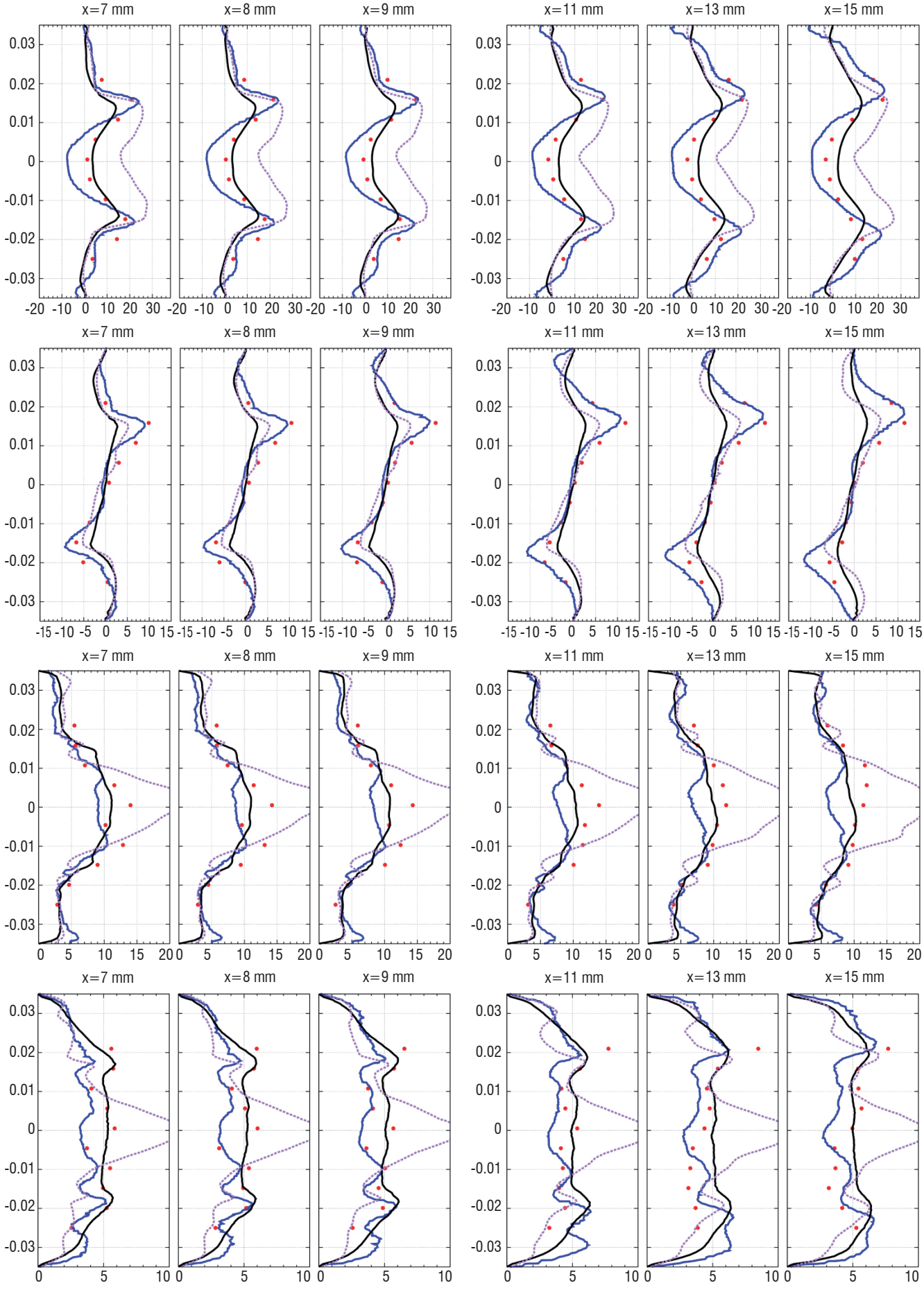

Figure 15 - Comparison of mean profiles. From top to bottom, axial, transverse mean velocities and axial, transverse rms velocities

— : AVBP, — : CEDRE "-n", ···: CEDRE "-b4n2", ●: experiment

modes are filtered. The linear acoustic (Riemann) and entropy invariants are constructed in a second step, using Eqs. (1)-(3):

$$P^{+} = \frac{1}{2}\left(\frac{p'}{\overline{\gamma p}} + \frac{u'}{\overline{c}}\right)$$

downstream propagating acoustic wave (velocity $\overline{u} + \overline{c}$) (1)

$$P^{-} = \frac{1}{2}\left(\frac{p'}{\overline{\gamma p}} - \frac{u'}{\overline{c}}\right)$$

upstream propagating acoustic wave (velocity $\overline{u} - \overline{c}$) (2)

$$\sigma = \frac{s'}{c_p}$$ entropy wave (velocity $\overline{u}$) (3)

These invariants still contain spurious contributions that come from the turbulence of the flow. In order to get rid of this turbulent contamination, a phase averaging of each invariant is finally performed by taking into account the different propagation velocities of the waves between the planes.

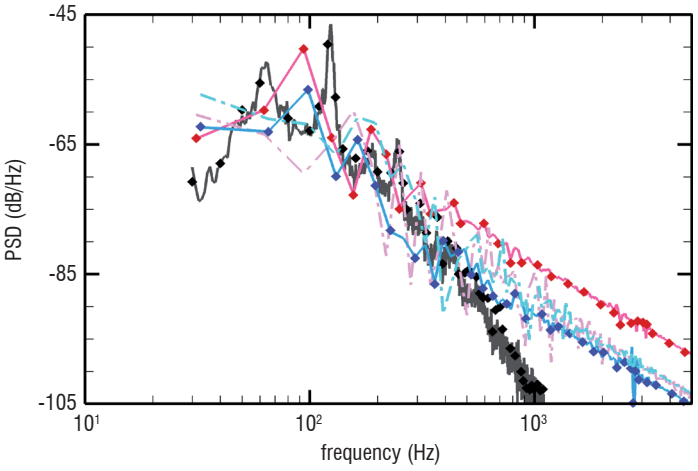

Figure 17 - Power spectral densities of the simulated invariants inside the combustion chamber (the reference amplitude is set to 1 for all invariants)

CEDRE: P_1^+ ; P_1^- ; σ_1

AVBP: P_1^+ ; P_1^- ; σ_1

Experiments: P_1^+ ; P_1^-

The wave extraction procedure is applied to the unsteady fields computed by CEDRE and AVBP. It must be mentioned here that P_1^+ corresponds to the wave propagating toward the nozzle and does not identify with the direct combustion noise generated by the flame, since it also includes reflections of P_1^- on the flame and on the combustor upstream boundary. The power spectral densities of the three invariants extracted from both simulations are reproduced in Figure 17, where the experimental acoustic invariants are also reproduced. The two computations exhibit a similar spectral content for the acoustic waves, with the most energetic fluctuations located in the low-frequency region. In particular, the levels of the two waves are identical, which indicates that the nozzle fully reflects the acoustic perturbations. In the experiments, the faster decrease of the levels above 300 Hz may arise from a limitation of the wave separation method due to the limited spatial resolution of the measurements.

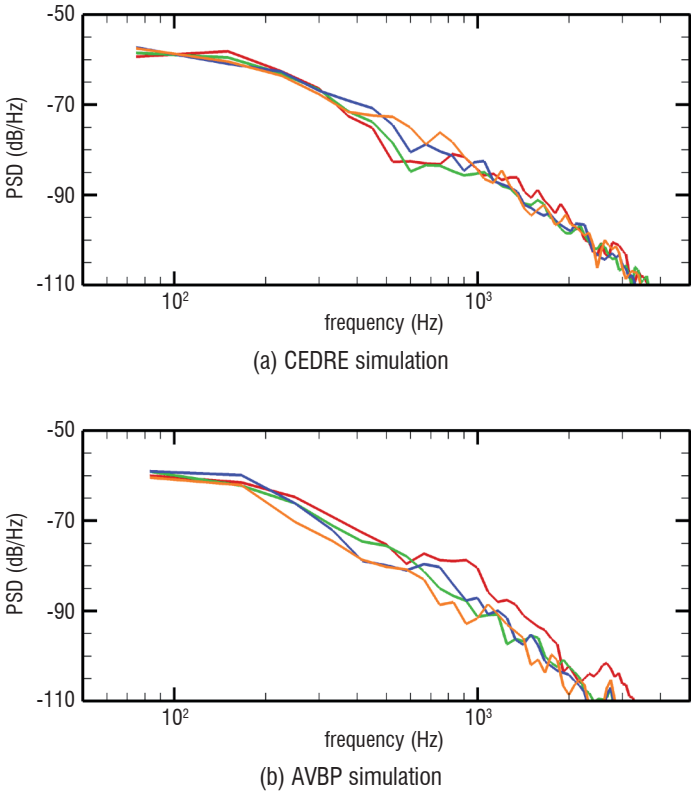

Figure 18 - Power spectral densities of the entropy invariant at various locations in the combustion chamber
x = 0.0875 m; x = 0.1015 m; x = 0.1155 m; x = 0.1295 m

Finally, the nondimensionalized entropy fluctuations generated by the flame are very similar to the acoustic ones, with the amplitude of the fluctuations decreasing with the increasing frequency.

The phase averaging performed to get rid of the turbulent contamination of the signals considers that the waves propagate without dissipation or diffusion. This hypothesis is well verified for the acoustic waves, however distortions may occur for the entropy waves, due for instance to the turbulent mixing. The power spectral densities of the entropy fluctuation on different storage planes, before the phase averaging, are illustrated in Figure 18. The energetic frequencies correspond to the large length scales ($\lambda \sim 10$ cm at 100 Hz), a length similar to that of the combustion chamber. Mixing and diffusion are therefore negligible at these low frequencies, as can be seen in the figure. The attenuation of the entropy fluctuations remains limited for all of the frequencies of interest, in particular for the CEDRE simulation. A slightly more important attenuation can be seen for AVBP, but still remains low. This figure also proves that the grids are sufficiently dense to convect the entropy wave without noticeable numerical dissipation.

Noise generation through the nozzle

At the end of the combustion chamber, the downstream acoustic wave and the entropy wave are accelerated through the nozzle. For the acoustic wave, this causes sound scattering with an attenuation of the acoustics transmitted through the nozzle, while some noise is reflected to the chamber; for the entropy wave, the flow acceleration generates indirect noise, both upstream and downstream from the nozzle. Marble & Candel were the first to provide an analytical model to account for both phenomena [17], by writing conservation

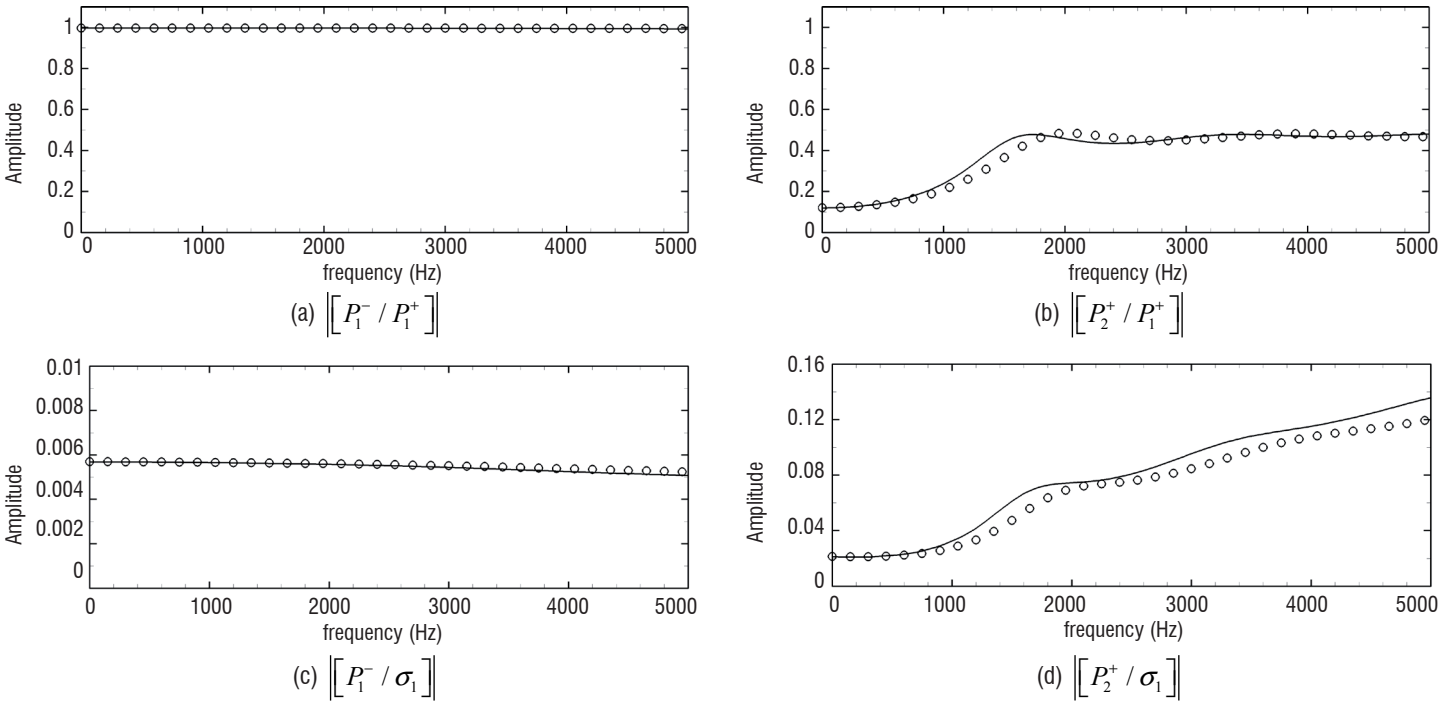

Figure 19 - Amplitude of the (a), (b) acoustic and (c), (d) thermoacoustic transfer functions of the nozzle – MarCan; ○ Anozzle

relations for the fluctuations of mass, stagnation temperature and entropy through the nozzle. This approach assumes that the nozzle is compact with respect to the considered harmonic perturbations, which limits its validity to low frequencies only. Even if combustion noise is assumed to lay in a rather low frequency range, the compact hypothesis seems too restrictive for real engines, and non-compact models are required for a correct estimation of the generated noise. A first linear model was proposed by Marble & Candel [17] for a supercritical nozzle with a linear velocity profile. They reduced the linearized Euler equations to a simple hypergeometric differential equation over the pressure, using a nondimensionalization based on the constant velocity gradient. Their approach was recently extended to piecewise-linear velocity profiles by Giauque *et al* [72] and to shocked nozzles by Moase *et al* [73], so that any nozzle geometry and flow condition can be modeled. This generalization relies on the resolution of a matrix system using the analytical expressions for the pressure, velocity and entropy perturbations in each element (as solutions of the hypergeometric differential equation) and continuity relations between two elements or through the shock. Following a different approach, Duran & Moreau [74] recast the linearized Euler Equations to write a differential system over the fluctuations of mass flow rate, stagnation temperature and entropy, which is solved using the Magnus expansion. Here again, the presence of a shock wave is addressed by using jump relations derived from Rankine and Hugoniot.

All of the above-mentioned models deal with a 1D mean flow and perturbations. However, as pointed out by Zheng *et al* [75], those models fail to reproduce the experimental results of Bake *et al* [32] for a subcritical nozzle, and a possible reason for their failure seems to be the experimental distortion of the entropy wave, which is not taken into account by the 1D models. Indeed, in practical cases, the velocity profile is not uniform over a section and the radial gradient of the axial velocity deforms the initially planar entropy front while being convected through the nozzle, thus modifying the indirect noise generation process. Zheng *et al* [75] extended the 1D models to 2 dimensional flows, in order to take into account this heterogeneous radial velocity profile, while Ullrich & Sattelmayer [76], [77] used linearized Navier-Stokes equations to evaluate the nozzle transfer functions numerically.

As an illustration, the analytical evaluation of the nozzle transfer functions obtained with the 1D models of ONERA (piecewise-linear velocity profile, MarCan code) and CERFACS (Magnus expansion, ANozzle code) are reproduced in Figure 19 for the nozzle located at the downstream end of the CESAM-HP combustion chamber (Subscripts 1 and 2 refer to values at the nozzle inlet and outlet). The nozzle is supercritical and a normal shock is located in the diffuser. The Mach numbers at the nozzle inlet and nozzle outlet are $\overline{M}_1 = 0.011$ and $\overline{M}_2 = 0.046$, respectively. The nozzle geometry and mean Mach number profile are reproduced in Figure 20. It has been verified with RANS and LES simulations, not presented here, that the flow remains attached in the diffuser, so the predictions of the 1D isentropic models are valid.

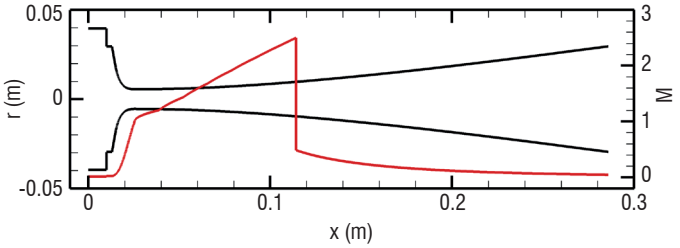

Figure 20 - Nozzle geometry and mean Mach number profile
nozzle walls (left axis); Mach profile (right axis)

Let us first discuss the noise reflections through the nozzle (waves P_1^- generated by acoustic and entropy forcings). Due to the choked nozzle configuration, only the converging part of the nozzle contributes to this noise. The converging nozzle being of small size, its response is essentially compact and does not vary for the considered frequencies. The converging nozzle is fully reflective for inlet acoustic disturbances, whereas the upstream-propagating noise generated by entropy perturbations is very low. The amplitude ratio of the transfer functions between the acoustic-generated and entropy-generated noise is over 150. Note that this ratio does not strictly correspond to the ratio between the scattered direct combustion noise and the entropy-generated noise (indirect combustion noise), since P_1^+ already includes entropy-generated noise through the reflection of P_1^- on the upstream boundary of the combustor.

Considering now the noise transmission through the nozzle (waves P_2^+), the length of the diverging part being largely higher than that of the converging one, the non-compactness of the nozzle on the generated noise is more visible for the downstream wave. For frequencies above 600 Hz, the nozzle is no longer compact and the amplitude of the nozzle response to the acoustic and entropy forcings increases. Once again, the amplitude of the acoustic-generated noise transfer function is larger than that of the entropy, but the ratio is limited to 5, a value much lower than for the upstream wave. The presence of a transmitted acoustic wave may seem unphysical at first sight, given that the nozzle is fully reflective for inlet acoustic disturbances. This paradox is solved by considering the energy of the waves. Indeed, the transfer functions deal with pressure fluctuations non-dimensionalised by the mean pressure, a quantity that is not conserved by the flow. In the present case, full reflection of the incident pressure fluctuations corresponds to a reflected acoustic energy below 1, because of the presence of the mean flow (see for instance [78]), leading to the transmission of some part of the acoustic energy.

Application to the combustion chamber

Once the characteristic waves inside the combustion chamber and the nozzle transfer functions are known, it is straightforward to analytically evaluate the noise scattered by (direct contribution) and produced inside (indirect contribution) the nozzle, and that returning inside the chamber or entering the turbine stages. This evaluation is performed in the spectral domain using Eqs. (4)-(5)

$$P_1^- = \left[\frac{P_1^-}{P_1^+}\right] P_1^+ + \left[\frac{P_1^-}{\sigma_1}\right] \sigma_1 \qquad (4)$$

$$P_2^+ = \left[\frac{P_2^+}{P_1^+}\right] P_1^+ + \left[\frac{P_2^+}{\sigma_1}\right] \sigma_1 \qquad (5)$$

where the terms in brackets correspond to the nozzle transfer functions and the perturbations incoming from the downstream part of the nozzle are assumed to be nil ($P_2^- = 0$).

The spectra of the waves P_1^- and P_2^+ evaluated numerically and analytically are reproduced in Figure 21. The results are very similar for the 2 simulations. The analytical spectrum of P_1^- collapses perfectly with the simulated one, which is a first validation of the approach applied here for the analytical reconstruction of the noise emitted by the nozzle. Given that the incoming acoustic and entropy fluctuations are of the same order and that the amplitude of the acoustic transfer function is 150 times larger than the thermo-acoustic one, the wave P_1^- comes exclusively from the scattering of P_1^+ through the nozzle. However, this result does not strictly demonstrate that direct noise dominates indirect noise, since P_1^+ does not identify with direct combustion noise because it includes reflections of P_1^- on the upstream boundary of the combustor.

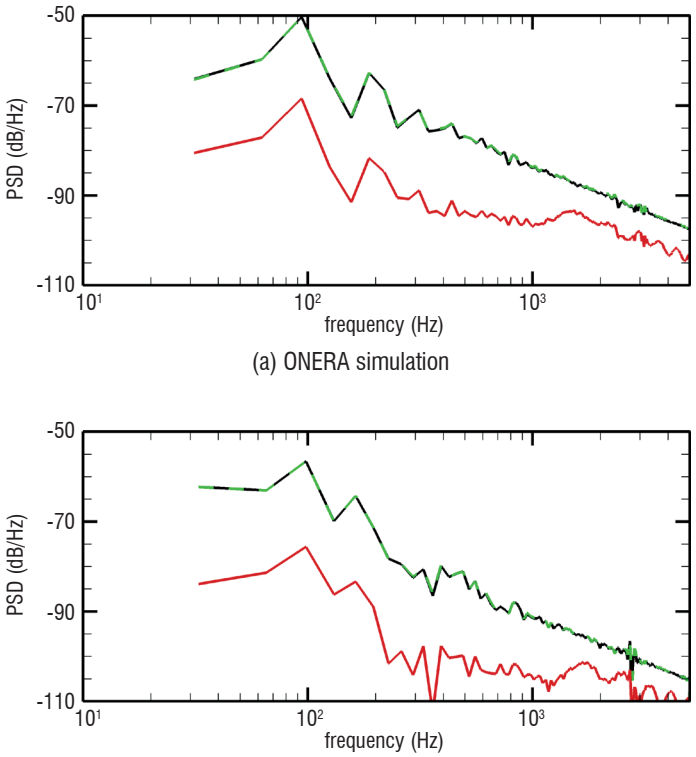

Figure 21 - Spectra of the acoustic invariants leaving the nozzle
— P_1^- from CFD; ··· P_1^- from analytical methods; — P_2^+ from analytical methods

In the present CFD simulations, the nozzle is choked and the region downstream from the throat is not represented in the numerical domain, which focuses on the flow inside the combustion chamber. It is therefore not possible to determine the amplitude of the downstream acoustic wave from the CFD, but this wave can be reconstructed using the analytical model. From the levels of the invariants inside the chamber and the amplitudes of the transfer functions, it is obvious that the downstream noise comes essentially from the transmission of the wave P_1^+ through the nozzle, with a very limited contribution of the entropy source. Given that the levels of the acoustic transfer function $\left[P_2^+ / P_1^+\right]$ are lower than that of $\left[P_1^- / P_1^+\right]$, the downstream acoustic wave exhibits levels below those of the upstream wave, from -18 dB in the low frequencies to -7 dB above 2 kHz. It may appear surprising that entropy-generated noise remains negligible compared to transmitted acoustics downstream from the nozzle, since incident acoustic and entropy waves exhibit similar levels and most of the incident acoustic energy is reflected to the combustion chamber. The thermo-acoustic transfer functions in Figure 19, however, indicate that energy conversion from entropy to acoustics is very limited in the present case. A detailed look at the compact response

(low-frequency limit) of nozzles to entropy forcing (see [73], [79]) indicates that this behavior is observed for almost all shocked nozzle regimes.

Conclusions and perspectives

With the important reduction of jet and fan noise achieved for recent turbojet engines, combustion noise now starts to emerge and attention must be focused on its understanding and reduction. The objective of the European project RECORD, run between 2013 and 2015, was to improve the global knowledge of the fundamental mechanisms of core noise generation, in order to provide tools for its evaluation and to propose ways for its reduction. To this end, the high-pressure combustor CESAM-HP has been built at EM2C laboratory, in order to experimentally investigate combustion noise and its contributors – direct (acoustic) and indirect (entropy) combustion noises. The facility features a one-staged swirl injector, a combustion chamber and an exhaust nozzle used to pressurize the combustion chamber and generate indirect noise. Special care has been taken to allow various diagnostic techniques to quantify the flow properties and acoustics, such as temperature and pressure measurements or large optical accesses inside the chamber. Numerical simulations of the reactive experiment have been conducted at ONERA and at CERFACS with different solvers. They have been shown to reproduce the experimental characteristics of the flame and the associated pressure fluctuations inside the chamber with a very good accuracy. In particular, it is remarkable that both codes produced results in close agreement with the measurements, as illustrated by the pressure time signal and PSD in the chamber and by the temperature data in the plenum domain. This gives good confidence in the ability of the HFLES approach to describe complex combustion chamber phenomena. Finally, an acoustic post-processing of the simulations has been performed to extract the waves present inside the combustion chamber (acoustic, entropy) and to propagate them through the nozzle, in order to model the direct and indirect contributions. The numerical method predicts the predominance of the direct contribution for the noise reflected by the nozzle, with the nozzle being fully reflective to the acoustic forcing. This behavior is confirmed by the comparison with the experiments. The numerical method also provides the noise transmitted by the nozzle and that is not measured experimentally. This information is of crucial importance for the modeling of a complete engine, where the fluctuations create additional noise when they are accelerated through the turbine stages.

Despite the differences with a real gas turbine combustor, the facility investigated in this paper exhibits some of its main characteristics and the demonstration that the numerical codes are able to capture combustion noise is an important step. Follow-up activities will require, for instance, liquid jet fuels and realistic combustion chambers to be considered. Noise modeling through a turbine is also a key issue for the correct prediction of combustion noise. In addition to the combustor test case, a full stator-rotor stage has been instrumented at the university *Politecnico di Milano* within the framework of RECORD, with various types of acoustic, entropic or vortical excitations. This facility is of prime interest for the experimental validation of turbine models. The coupling of the analytical models representing the various engine elements with the numerical simulation of the combustor will provide, in the end, the combustion noise radiated to the ground and will help to understand the relative contributions of the contributors, in order to finally design quieter aircraft ■

Acknowledgements

The numerical results were obtained during the RECORD project (Research on Core Noise Reduction). RECORD is a project funded by the European Union within the framework of the Seventh Framework Program (FP7/2007- 2013), under Grant Agreement No. 312444.

References

[1] A. P. DOWLING, Y. MAHMOUDI - *Combustion Noise*. Proceedings of the Combustion Institute, 35:65-100 (2015).

[2] W. C. STRAHLE - *A Review of Combustion Generated Noise*. 1st AIAA Aeroacoustics Conference, Paper AIAA 73-1023 (1973).

[3] D. G. CRIGHTON - *The Excess Noise Field of Subsonic Jets*. Journal of Fluid Mechanics, 56:683-694 (1972).

[4] N. A. CUMPSTY, F. E. MARBLE - *Core Noise from Gas Turbine Exhausts*. Journal of Sound and Vibration, 54:297–309 (1977).

[5] W. C. STRAHLE - *Combustion Noise*. Progress in Energy and Combustion Science, 4:157–176 (1978).

[6] S. BRAGG - *Combustion Noise*. Journal of the Institute of Fuel, 36:12–16 (1963).

[7] W. STRAHLE - *On Combustion Generated Noise*. Journal of Fluid Mechanics, 49:399–414 (1971).

[8] T. SMITH, J., KILHAM - *Noise Generated by Open Turbulent Flame*. Journal of the Acoustical Society of America, 35:715–724 (1963).

[9] A. THOMAS, G. WILLIAMS - *Flame Noise: Sound Emission From Spark-ignited Bubbles of Combustible Gas.* Proceedings of the Royal Society London A, 294:449–466 (1966).

[10] I. HURLE, R. PRICE, T. SUDGEN, A. THOMAS - *Sound Emission From Open Turbulent Flames*. Proceedings of the Royal Society London A, 303:409–427 (1968).

[11] W. STRAHLE - *Some Results in Combustion Generated Noise*. Journal of Sound and Vibration, 23:113–125 (1972).

[12] W. STRAHLE - *Refraction, Convection, and Diffusion Flame Effects in Combustion-Generated Noise*. Proceedings of the Combustion Institute, Pittsburgh, pp. 527–535 (1973).

[13] A. DOWLING, J. E. FFWOCS WILLIAMS - *Sound and Sources of Sound*. Ellis Horwood, Chichester, UK (1983).

[14] S. M. CANDEL - *Analytical Studies of Some Acoustic Problems of Jet Engines*. PhD thesis, California Institute of Technology, Pasadena (1972).

[15] F. E. MARBLE - *Acoustic Disturbance From Gas Non-Uniformities Convecting Through a Nozzle*. In Interagency Symposium on University Research in Transportation Noise, Stanford University, Stanford, CA, pp. 547–561 (1973).

[16] C. L. MORFEY - *Amplification of Aerodynamic Noise by Convected Flow Inhomogeneities*. Journal of Sound and Vibration, 31:391–397 (1973).

[17] F. E. MARBLE, S. M. CANDEL - *Acoustic Disturbance From Gas Non-Uniformities Convected Through a Nozzle*. Journal of Sound and Vibration 55:225-243 (1977).

[18] N. A. CUMPSTY, F. E. MARBLE - *The Interaction of Entropy Fluctuations With Turbine Blade Rows: a Mechanism of Turbojet Engine Noise*. Proceedings of the Royal Society of London A, 357:323–344 (1977).

[19] S. CANDEL - *Combustion Instabilities Coupled by Pressure Waves and Their Active Control*. Proceedings of the Combustion Institute, 24:1277–1296 (1992).

[20] F. CULICK, V. YANG - *Progress in Astronautics and Aeronautics: Liquid Rocket Engine Combustion Instability*. Vol. 169. AIAA, Ch. 1: Overview of combustion instabilities in liquid-propellant rocket engines, pp. 3–37 (1995).

[21] S. CANDEL - *Combustion Dynamics and Control: Progress and Challenges*. Proceedings of the Combustion Institute, 29:1–28 (2002).

[22] T. LIEUWEN, V. YANG (Eds.) - *Combustion Instabilities in Gas Turbine Engines: Operational Experience*. Fundamental Mechanisms, and Modeling, Progress in Astronautics and Aeronautics, Volume 210, AIAA, Washington (2005).

[23] A. GIAUQUE - *Fonctions de transfert de flamme et énergies de perturbation dans les écoulements réactifs*. PhD Thesis, *Institut National Polytechnique de Toulouse*, Toulouse, France (2007).

[24] M. J. BREAR, F. NICOUD, M. TALEI, A. GIAUQUE, E. R. HAWKES - *Disturbance Energy Transport and Sound Production in Gaseous Combustion*. Journal of Fluid Mechanics, 707:53-73 (2012).

[25] C. S. GOH, A. S. MORGANS - *The Influence of Entropy Waves on the Thermoacoustic Stability of a Model Combustor*. Combustion Science and Technology, 185:249-268 (2013).

[26] S. HOCHGREB, D. DENNIS, I. AYRANCI, W. BAINBRIDGE, S. CANT - *Forced and Self-excited Instabilities from Lean Premixed, Liquid-Fuelled Aeroengine Injectors at High Pressures and Temperatures*. In Proceedings of ASME Turbo Expo, Paper GT2013-95311 (2013).

[27] E. MOTHEAU, Y. MERY, F. NICOUD, T. POINSOT - *Analysis and Modeling of Entropy Modes in a Realistic Aeronautical Gas Turbine*. Journal of Engineering for Gas Turbines and Power, 135:092602 (2013).

[28] E. MOTHEAU, F. NICOUD, T. POINSOT - *Mixed Acoustic-Entropy Combustion Instabilities in Gas Turbines*. Journal of Fluid Mechanics 749:542-576 (2014).

[29] S. CANDEL, D. DUROX, S. DUCRUIX, A.-L. BIRBAUD, N. NOIRAY, T. SCHULLER - *Flame Dynamics and Combustion Noise: Progress and Challenges*. International Journal of Aeroacoustics, 8:1-56 (2009).

[30] K. R. MCMANUS, T. POINSOT, S. M. CANDEL - *A Review of Active Control of Combustion Instabilities*. Progress in Energy and Combustion Science, 19:1-29 (1993).

[31] I. DURAN, S. MOREAU, F. NICOUD, T. LIVEBARDON, E. BOUTY, T. POINSOT - *Combustion Noise in Modern Aero-Engines*. Aerospace Lab, 7 (2014).

[32] F. BAKE, C. RICHTER, B. MÜLHBAUER, N. KINGS, I. RÖHLE, F. THIELE, B. NOLL - *The Entropy Wave Generator (EWG): a Reference Case on Entropy Noise*. Journal of Sound and Vibration, 326:574-598 (2009).

[33] B. PARDOWITZ, U. TAPKEN, K. KNOBLOCH, F. BAKE, E. BOUTY, I. DAVIS, G. BENNETT - *Core Noise – Identification of Broadband Noise Sources of a Turbo-Shaft Engine*. 20th AIAA/CEAS Aeroacoustics Conference, Paper AIAA 2014-3321 (2014).

[34] D. BLACODON, S. LEWY - *Source Localization of Turboshaft Engine Broadband Noise Using a Three-Sensor Coherence Method*. Journal of Sound and Vibration, 338:250-262 (2015).

[35] F. BAKE, K. KNOBLOCH - *Research on Core Noise Reduction*. AeroDays 2015, London (2015)

[36] K. KNOBLOCH, T. WERNER, F. BAKE - *Noise Generation in hot Nozzle Flow*. Proceedings of ASME Turbo Expo, Paper GT2015-43702 (2015).

[37] K. KNOBLOCH, T. WERNER, F. BAKE - *Entropy Noise Generation and Reduction in a Heated Nozzle Flow*. 21st AIAA/CEAS Aeroacoustics Conference, Paper AIAA 2015-2818 (2015).

[38] M. MAZUR, W. TAO, P. SCOUFLAIRE, F. RICHECOEUR, S. DUCRUIX - *Experimental and Analytical Study of the Acoustic Properties of a Gas Turbine Model Combustor with a Choked Nozzle*. Proceedings of ASME Turbo Expo, Paper GT2015-43013 (2015).

[39] L. PINELLI, F. POLI, A. ARNONE, S. GUÉRIN, A. HOLEWA, J. R. F. APARICIO, R. PUENTE, D. TORZO, C. FAVRE, P. GAETANI, G. PERSICO - *On the Numerical Evaluation of Tone Noise Emissions Generated by a Turbine Stage: an In-Depth Comparison Among Different Computational Methods*. Proceedings of ASME Turbo Expo, Paper GT2015-42376 (2015).

[40] N. TRAN, S. DUCRUIX, T. SCHULLER - *Damping Combustion Instabilities with Perforates at the Premixer Inlet of a Swirled Burner*. Proceedings of the Combustion Institute 32:2917–2924 (2009).

[41] A. SCARPATO - *Linear and Nonlinear Analysis of the Acoustic Response of Perforated Plates Traversed by a Bias Flow*. PhD Thesis, *Ecole Centrale Paris* (2014).

[42] A. GIAUQUE, M. HUET, F. CLERO, S. DUCRUIX, F. RICHECOEUR - *Thermoacoustic Shape Optimisation of a Subsonic Nozzle*. Journal of Engineering for Gas Turbines and Power, 135:102601 (2013).

[43] J.-F. BROUCKAERT, M. MERSINLIGIL, M. PAU - *A Conceptual Design Study for a New High Temperature Fast Response Cooled Total Pressure Probe*. Proceedings of the ASME Turbo Expo 2008 Power for Land, Sea and Air, June 9-13, 2008, Berlin, Germany (2008).

[44] M. MERSINLIGIL, J.-F. BROUCKAERT, J. DESSET - *First Unsteady Pressure Measurements with a Fast Response Cooled Total Pressure Probe in High Temperature Gas Turbine Environments*. Proceedings of the ASME Turbo Expo 2010 Power for Land, Sea and Air, June 14-18, 2010, Glasgow, UK (2010).

[45] M. MERSINLIGIL, J. DESSET, J.-F. BROUCKAERT - *High Temperature High Frequency Turbine Exit Flow Field Measurements in a Military Engine with a Cooled Unsteady Total Pressure Probe*. Proceedings of the Institution of Mechanical Engineers, Part A: Journal of Power and Energy (2011).

[46] M. MAZUR, N. KINGS, P. SCOUFLAIRE, F. RICHECOEUR, S. DUCRUIX - *Combustion Noise Studies of a Swirled Combustion Chamber with a Choked Nozzle Using High-Speed Diagnostics*. X-NOISE Workshop 2015, La Rochelle, France (2015).

[47] N. KINGS, W. TAO, P. SCOUFLAIRE, F. RICHECOEUR, S. DUCRUIX - *Experimental and Numerical Investigation of direct and Indirect Combustion Noise Contributions in a Lean Premixed Laboratory Swirled Combustor*. Proceedings of ASME Turbo Expo, Paper GT2016-57848 (2016).

[48] T. SCHÖNFELD, M. RUDGYARD - *Steady and Unsteady Flow Simulations Using the Hybrid Flow Solver AVBP.* AIAA Journal, 37:1378-1385 (1999). doi:10.2514/2.636. http://arc.aiaa.org/doi/abs/10.2514/2.636.

[49] V. MOUREAU, G. LARTIGUE, Y. SOMMERER, C. ANGELBERGER, O. COLIN, T. POINSOT - *Numerical Methods for Unsteady Compressible Multi-Component Reacting Flows on Fixed and Moving Grids*. Journal of Computational Physics, 202:710-736 (2015).

[50] Cerfacs - *The AVBP HandBook (2008)*. http://www.cerfacs.fr/avbp7x//RESOURCES/HTML/main.html.

[51] O. COLIN, M. RUDGYARD - *Development of High-Order Taylor-Galerkin Schemes for LES*. Journal of Computational Physics, 162:338-371 (2000).

[52] F. NICOUD, H. B. TODA, O. CABRIT, S. BOSE, J. LEE - *Using Singular Values to Build a Subgrid-Scale Model for Large Eddy Simulations*. Physics of Fluids 23:085106 (2011).

[53] J. P. LEGIER, T. POINSOT, D. VEYNANTE - *Dynamically Thickened Flame LES Model for Premixed and Non-Premixed Turbulent Combustion*. Proceedings of the Summer Program: 157-168 (2011).

[54] F. CHARLETTE, C. MENEVEAU, D. VEYNANTE - *A Power-Law Flame Wrinkling Model for LES of Premixed Turbulent Combustion Part I: Non-Dynamic Formulation and Initial Tests*. Combustion and Flame 131:159–180 (2002).

[55] T. J. POINSOT, S. K. LELE - *Boundary Conditions for Direct Simulations of Compressible Viscous Flows*. Journal of Computational Physics 101:104–129 (1992).

[56] S. MENDEZ, J. D. ELDREDGE - *Acoustic Modeling of Perforated Plates with Bias Flow for Large-Eddy Simulations*. Journal of Computational Physics 228:4757–4772 (2009).

[57] A. REFLOCH, B. COURBET, A. MURRONE, P. VILLEDIEU, C. LAURENT, P. GILBANK, J. TROYES, L. TESSÉ, G. CHAINERAY, J.B. DARGAUD, E. QUÉMERAIS, F. VUILLOT - *CEDRE Software*. Aerospace Lab, 2 (2011).

[58] D. SCHERRER, F. CHEDEVERGNE, P. GRENARD, J. TROYES, A. MURRONE, E. MONTREUIL, F. VUILLOT, N. LUPOGLAZOFF, M. HUET, B. SAINTE-ROSE, P. THORIGNY, N. BERTIER, J.M. LAMET, T. LE PICHON, E. RADENAC, A. NICOLE, L. MATUSZEWSKI, M. ERRERA - Recent CEDRE applications. Aerospace Lab, 2 (2011).

[59] F. DUPOIRIEUX, N. BERTIER - *The Models of Turbulent Combustion in the CHARME Solver of CEDRE*. Aerospace Lab, 2 (2011).

[60] B. SAINTE-ROSE, N. BERTIER, S. DECK, F. DUPOIRIEUX - *A DES Method Applied to a Backward Facing Step Reactive Flow*. *Comptes Rendus Mécanique*, 337:340–351 (2009).

[61] M. LORTEAU, F. CLÉRO, F. VUILLOT - *Analysis of Noise Radiation Mechanisms in Hot Subsonic Jet from a Validated Large Eddy Simulation Solution*. Physics of Fluids 27:075108 (2015). doi: 10.1063/1.4926792

[62] F. HAIDER, J.-P. CROISILLE, B. COURBET - *Stability of the Cell Centered Finite-Volume MUSCL Method on Unstructured Grids*. *Numerische Mathematik*, 113:555-600 (2009).

[63] S. DECK - *Recent Improvements in the Zonal Detached Eddy Simulation (ZDES) Formulation*. Theoretical and Computational Fluid Dynamics, 26:523–550 (2012).

[64] F. VUILLOT, N. LUPOGLAZOFF - *Combustion and Turbulent Flow Effects in 2D Unsteady Navier-Stokes Simulations of Oscillatory Rocket Motors*. 34th AIAA Aerospace Sciences Meeting, paper 96-0884 (1996).

[65] N. LUPOGLAZOFF, F. VUILLOT - *Simulations of Solid Propellant Rocket Motors Instability Including Propellant Combustion Response*. 6th International Congress on Sound and Vibration (1999).

[66] Centaur grid generation software: https://www.centaursoft.com.

[67] C. J. LAPEYRE, M. MAZUR, P. SCOUFLAIRE, F. RICHECOEUR, S. DUCRUIX, T. POINSOT - *Acoustically Induced Vortex Core Flashback in a Staged Swirl-Stabilized Combustor*. Submitted to Flow, Turbulence and Combustion.

[68] C. LAPEYRE - *Étude numérique de la stabilité, la stabilisation et le bruit de flamme dans un brûleur tourbillonnaire en conditions amorcées*. PhD thesis, *Institut National Polytechnique de Toulouse*, Toulouse, France (2015).

[69] W. TAO - *Time Resolved Temperature and Pressure Based Methodology for Direct and Indirect Combustion Noise Separation*, PhD thesis, CentraleSupélec (2016).

[70] I. DURAN, M. LEYKO, S. MOREAU, F. NICOUD, T. POINSOT - *Computing Combustion Noise by Combining Large Eddy Simulations with Analytical Models for the Propagation of Waves Through Turbine Blades*. Compte Rendus Mecanique, 341:131-140 (2013).

[71] J. KOPITZ, E. BRÖCKER, W. POLIFKE - *Characteristics-Based Filter for Identification of Planar Acoustic Waves in Numerical Simulation of Turbulent Compressible Flow*. 12th International Congress on Sound and Vibration (2005).

[72] A. GIAUQUE, M. HUET, F. CLERO - *Analytical Analysis of Indirect Combustion Noise in Subcritical Nozzles*. Journal of Engineering for Gas Turbines and Power, 134:111202 (2012).

[73] W. H. MOASE, M. J. BREAR, C. MANZIE - *The Forced Response of Choked Nozzles and Supersonic Diffusers*. Journal of Fluid Mechanics, 585:281-304 (2007).

[74] I. DURAN, S. MOREAU - *Solution of the Quasi-One-Dimensional Linearized Euler Equations Using Flow Invariants and the Magnus Expansion*. Journal of Fluid Mechanics, 723:190-231 (2013).

[75] J. ZHENG, M. HUET, F. CLÉRO, A. GIAUQUE, S. DUCRUIX - *A 2D-Axisymmetric Analytical Model for the Estimation of Indirect Combustion Noise in Nozzle Flows*. 21st AIAA/CEAS Aeroacoustics Conference, Paper AIAA 2015-2974 (2015).

[76] W. C. ULLRICH, J. GIKADI, C. JÖRG, T. SATTELMAYER - *Acoustic-Entropy Coupling Behavior and Acoustic Scattering Properties of a Laval Nozzle*. 20th AIAA/CEAS Aeroacoustics Conference, Paper AIAA 2014-3193 (2014).

[77] W. C. ULLRICH, T. SATTELMAYER - *Transfer Functions of Acoustic, Entropy and Vorticity Waves in an Annular Model Combustor and Nozzle for the Prediction of the Ratio Between Indirect and Direct Combustion Noise*. 21st AIAA/CEAS Aeroacoustics Conference, Paper AIAA 2015-2972 (2015).

[78] K. KNOBLOCH, T. WERNER, F. BAKE - *Noise Generation in Hot Nozzle Flow*. Proceedings of ASME Turbo Expo 2015, Paper GT2015-43702 (2015).

[79] M. HUET - *Nonlinear Indirect Combustion Noise for Compact Supercritical Nozzle Flows*. Journal of Sound and Vibration, 374:211-227 (2016). http://dx.doi.org/10.1016/j.jsv.2016.03.028

Acronyms

CERFACS	(*Centre Européen de Recherche et de Formation Avancée en Calcul Scientifique)*
CESAM-HP	(*Combustion Etagée Swirlée Acoustiquement Maîtrisée - Haute Pression)*
DDES	(Delayed Detached Eddy Simulation)
DNS	(Direct Numerical Simulation)
EM2C	(*laboratoire d'Énergétique Moléculaire et Macroscopique, Combustion)*
HFLES	(High-Fidelity compressible Large Eddy Simulations)
ICS	(Impedance Control System)
IFP-EN	(*Institut Français du Pétrole - Energies nouvelles)*
LES	(Large Eddy Simulations)
ONERA	(*Office National d'Études et de Recherches Aérospatiales)*
PIV	(Particle Image Velocimetry)
PSD	(Power Spectral Density)
RANS	(Reynolds Averaged Navier Stokes)
RECORD	(REsearch on Core nOise ReDuction)
ZDES	(Zonal Detached Eddy Simulation)

AUTHOR

Maxime Huet graduated from Ecole Centrale Lyon in 2006 and received a Master degree in Acoustics from Lyon University the same year. He joined Onera in 2007 as a research scientist. His work is mainly dedicated to jet noise simulation and combustion noise modeling for their possible reduction.

Nicolas Bertier, graduated from ENS Cachan and PhD from Paris VI University, is senior researcher in the Energetics department of ONERA. He is project manager of CEDRE, which is the ONERA's code for energetics. His research activities focused on numerical simulations of reactive flows. He is also teaching combustion at Paris VI University and ISAE/Supaero (Toulouse).

François Vuillot graduated from Sup'Aero in 1981 and from U. of Washington in 1982. He is presently Scientific Advisor for complex simulations at the Fundamental and Applied Energetics Department of ONERA. He has been involved in unsteady numerical simulations for analyzing solid propellant rocket motor stability and jet noise for several years. He received the French "Académie des Sciences" Edmond Brun prize in 2008.

Marek Mazur graduated from RWTH Aachen University and Ecole Centrale Paris in 2013. He is a PhD student working on experimental studies of direct and indirect combustion noise in an aircraft type combustion chamber at EM2C Laboratory of CentraleSupélec and CNRS.

Nancy Kings has Ph.D. degree from TU Berlin. After her research assistant period at German Aerospace Center (DLR) she joined laboratoire EM2C of CNRS and CentraleSupélec as postdoctoral researcher focusing on combustion noise and on temperature measurement techniques.

Wenjie Tao graduated from Ecole Centrale de Pékin and Ecole Centrale Paris in 2011 and received her Ph.D. Degree on Combustion in 2016. Her Ph.D. thesis was on temperature and pressure measurements based methodology for direct and indirect combustion noise separation. She is now working as combustion and heat transfer engineer in ACAE.

Philippe Scouflaire is a CNRS Research Engineer in combustion, optical diagnostics, time resolved.

Franck Richecoeur has a PhD from Ecole Centrale Paris and a "Habilitation à Diriger des Recherches" from Université de Rouen. He is Lecturer at CentraleSupélec, where his activities are dedicated to experimental research on combustion instabilities, combustion noise, micro-combustion and processing of temporal data for the description of dynamical phenomena.

Sébastien Ducruix, laboratoire EM2C, CNRS, CentraleSupélec, Université Paris-Saclay. Engineering Degree, Master's Degree and PhD from Ecole Centrale Paris, "Habilité à Diriger des Recherches" (HDR) from Institut National Polytechnique de Toulouse. Sébastien Ducruix is Directeur de Recherche at the CNRS and presently Deputy Director of EM2C. His research activity mainly concerns the theoretical, experimental and numerical characterization of the dynamics of flames and fundamental mechanisms of combustion-acoustic interactions, in particular for gas turbines and rocket engines. Sébastien Ducruix is the scientific coordinator of the French-German collaborative program REST (Rocket Engine STability Initiative) set up by AIRBUS, CNES, DLR, ONERA and SAFRAN. He is Vanguard Chair for the Committee "Combustion, Fuel and Emission" of the international conference Turbine Technical Conference and Exposition -TurboExpo. He is Vice Chairman of the thematic area "Propulsion" for the ASTech cluster (Aeronautics and Space in Paris Region).

Corentin Lapeyre graduated from Ecole Centrale Lyon in 2011, and obtained a PhD in numerical combustion from INP Toulouse in 2015. His thesis work was performed at Cerfacs, and funded by the DISCERN ANR. It concerned compressible flame dynamics in pressurized systems, including flame noise and stability, as well as flashback. Since 2015 he is a Postdoctoral Fellow at IMFT, working on flame-vortex interactions for alternative fuels under the IDYLLE ANR grant.

Thierry Poinsot received his PhD thesis in heat transfer from Ecole Centrale Paris in 1983 and his Thèse d'Etat in combustion in 1987. He is a research director at CNRS, head of the CFD group at Cerfacs, senior research fellow at Stanford University and a consultant for various companies. After his thesis at Ecole Centrale Paris and after two years of post-doctoral work at Stanford, he started combustion activities at Cerfacs in 1992 and his group (60 persons in 2010) has produced a significant part of the recent research in the field of LES of turbulent combustion in gas turbines. He teaches numerical methods and combustion at many schools and universities (Ecole Centrale Paris, ENSEEIHT, Ensica, Supaero, UPS, Stanford, Von Karmann Institute, CEFRC Princeton and Beijing). He has authored more than 150 papers in refereed journals and 200 communications. He is the co-author of the textbook "Theoretical and numerical combustion" together with Dr D. Veynante and an associate editor of "Combustion and Flame". He received the first Cray prize in 1993, the BMW prize in 2002, the Grand Prix of the French Academy in 2003 and an ERC advanced grant in 2013.

Office National d'Études et de Recherches Aérospatiales
BP 72 - 29, Avenue de la Dicision Leclerc
92322 CHATILLON Cedex
Tél. : +33 1 46 73 40 40 - Fax : +33 1 46 73 41 41
http://www.onera.fr